



Open Access

INVITED ORIGINAL ARTICLE

Sperm Biology

Rescue of male infertility through correcting a genetic mutation causing meiotic arrest in spermatogonial stem cells

Ying-Hua Wang^{1,*}, Meng Yan^{1,*}, Xi Zhang^{2,*}, Xin-Yu Liu¹, Yi-Fu Ding¹, Chong-Ping Lai¹, Ming-Han Tong², Jin-Song Li^{1,3,4}

Azoospermia patients who carry a monogenetic mutation that causes meiotic arrest may have their biological child through genetic correction in spermatogonial stem cells (SSCs). However, such therapy for infertility has not been experimentally investigated yet. In this study, a mouse model with an X-linked testis-expressed 11 (*TEX11*) mutation (*Tex11^{PMY}*) identified in azoospermia patients exhibited meiotic arrest due to aberrant chromosome segregation. *Tex11^{PMY}* SSCs could be isolated and expanded *in vitro* normally, and the mutation was corrected by clustered regularly interspaced short palindromic repeats (CRISPR)–CRISPR-associated endonuclease 9 (Cas9), leading to the generation of repaired SSC lines. Whole-genome sequencing demonstrated that the mutation rate in repaired SSCs is comparable with that of autonomous mutation in untreated *Tex11^{PMY}* SSCs, and no predicted off-target sites are modified. Repaired SSCs could restore spermatogenesis in infertile males and give rise to fertile offspring at a high efficiency. In summary, our study establishes a paradigm for the treatment of male azoospermia by combining *in vitro* expansion of SSCs and gene therapy.

Asian Journal of Andrology (2021) 23, 590–599; doi: 10.4103/aja.aja_97_20; published online: 02 February 2021

Keywords: azoospermia; gene therapy; male infertility; meiotic arrest; spermatogonial stem cells; testis-expressed 11

INTRODUCTION

Male infertility is a complex pathological condition affecting around 7% of men of reproductive age.¹ Usually, infertile men can have their biological child through assisted reproductive technology (ART), such as intracytoplasmic sperm injection (ICSI), because these patients still have the ability to produce a small number of functional sperms for ART.² In contrast, it is impossible to restore fertility in men with nonobstructive azoospermia (NOA, approximately 10%–15% of all infertile males),³ the most clinically severe form of infertility which is defined by a complete absence of spermatozoa in the ejaculate and testis,⁴ through the currently available ARTs. Genetic studies reveal that NOA patients are at the highest risk of being carriers of genetic anomalies.¹ However, only a small fraction of NOA patients (around 20%) have established causal genetic diagnoses, including chromosomal aberrations (15%) and Y-chromosome azoospermia factor deletions.⁵

Recent efforts on unraveling the genetic causes for NOA through genome-wide approaches have led to the identification of single-gene mutations that account for spermatogenic failure.^{5–13} NOA patients carrying monogenic mutations causing spermatogenic failure^{14,15} may have substantial amount of functional spermatogonial stem cells (SSCs) in their testis.¹⁶ SSCs can self-renew and differentiate into mature sperm

in the seminiferous tubules, and can also be long-term expanded *in vitro* without losing their capacity to produce functional gametes *in vivo* after transplantation into recipient testis.^{16,17} Most importantly, the availability of SSCs offers the prospect for correction of a disease-causing genetic mutation by clustered regularly interspaced short palindromic repeats–CRISPR-associated endonuclease 9 (CRISPR-Cas9)-mediated homology-directed repair (HDR),^{18–20} which has been shown to be effective in repairing a cataract-causing genetic mutation in the SSCs isolated from a cataract mouse model.²¹ We thus reasoned that successful gene editing in SSCs carrying an azoospermia-causing mutation may resume the spermatogenesis of NOA patients. Moreover, *ex vivo* gene therapy in SSCs allows for selection of SSC lines with repaired gene and without unexpected mutations for transplantation through derivation of SSC lines from single-cell expansion followed by whole-genome sequencing.²¹ Therefore, gene therapy in cultured SSCs may potentially provide a chance for NOA patients with an identified single mutation to have their genetically related child without any unwanted genomic changes. However, the feasibility of infertility treatment by combined application of *in vitro* expansion of SSCs and gene therapy has not been investigated yet. In this study, we establish a strategy of patient-derived mutation xenocorrection (PDMX) to verify and correct a monogenic mutation that causes human azoospermia in mice.

¹State Key Laboratory of Cell Biology, Shanghai Key Laboratory of Molecular Andrology, Shanghai Institute of Biochemistry and Cell Biology, Center for Excellence in Molecular Cell Science, Chinese Academy of Sciences, University of Chinese Academy of Sciences, Shanghai 200031, China; ²State Key Laboratory of Molecular Biology, Shanghai Key Laboratory of Molecular Andrology, Shanghai Institute of Biochemistry and Cell Biology, Center for Excellence in Molecular Cell Science, Chinese Academy of Sciences, Shanghai 200031, China; ³School of Life Science and Technology, ShanghaiTech University, Shanghai 201210, China; ⁴School of Life Science, Hangzhou Institute for Advanced Study, University of Chinese Academy of Sciences, Hangzhou 310024, China.

*These authors contributed equally to this work.

Correspondence: Dr. MH Tong (minghan@sibcb.ac.cn) or Dr. JS Li (jsli@sibcb.ac.cn)

Received: 08 October 2020; Accepted: 02 December 2020

We chose *TEX11* gene to develop the PDMX model because *TEX11* mutations are recently revealed in NOA patients^{9,10,22} and *Tex11*-mutant mice resemble the patients' phenotypes of spermatogenic failure induced by meiotic arrest.^{23,24} The PDMX model basically includes the following steps: (1) generation of mouse models carrying NOA patient-originated *TEX11* mutations, (2) analysis of testicular phenotypes of males, (3) isolation and *in vitro* culture of SSCs, (4) correction of the genetic defect by CRISPR-Cas9-mediated HDR, (5) derivation of repaired SSC lines through single-cell expansion, (6) off-target effect analysis by whole-genome sequencing, (7) transplantation of the repaired SSCs into recipient testis to restore spermatogenesis, and (8) isolation of haploid gametes for fertility analysis. Here, we report the successful correction of an azoospermia patient-originated *TEX11* mutation and restoration of spermatogenesis in mice.

MATERIALS AND METHODS

Animal use and care

All animal procedures were performed under the ethical guidelines of the Institute of Biochemistry and Cell Biology, Shanghai Institute for Biological Sciences, Chinese Academy of Sciences (Shanghai, China).

Derivation of SSCs

To derive SSC lines, we sorted cells from testes of 8- to 10-day-old male mice using CD146. CD146⁺ cells were seeded on the mouse embryonic fibroblast (MEF) feeder cells and cultured with the modified SSC medium according to a previously reported protocol.

The culture medium consisted of StemPro-34 SFM (Invitrogen, Carlsbad, CA, USA) supplemented with StemPro supplement (Invitrogen), 25 $\mu\text{g ml}^{-1}$ insulin, 100 $\mu\text{g ml}^{-1}$ transferrin, 60 $\mu\text{mol l}^{-1}$ putrescine, 30 nmol l^{-1} sodium selenite, 6 mg ml^{-1} D-(+)-glucose, 30 $\mu\text{g ml}^{-1}$ pyruvic acid, 1 $\mu\text{l ml}^{-1}$ dl-lactic acid (Sigma, Saint Louis, MO, USA), 5 mg ml^{-1} bovine serum albumin (Sigma), 2 mmol l^{-1} L-glutamine (Millipore, Bedford, MA, USA), β -mercaptoethanol (Millipore), minimal essential medium vitamin solution (Invitrogen), nonessential amino acid solution (Millipore), penicillin/streptomycin (Invitrogen), 0.1 mmol l^{-1} ascorbic acid, 10 $\mu\text{g ml}^{-1}$ d-biotin (Sigma), 20 ng ml^{-1} recombinant human epidermal growth factor (Invitrogen), 10 ng ml^{-1} human basic fibroblast growth factor (Invitrogen), 10 ng ml^{-1} recombinant human glial cell line-derived neurotrophic factor (GDNF; Invitrogen), and 1% fetal bovine serum (FBS; ES cell-qualified, Invitrogen). The cells were maintained at 37°C in an atmosphere of 5% CO₂ in air. The culture medium was changed every 2–4 days. All the cultured cells were tested to ensure that they are mycoplasma free.

Plasmid construction

The CMV-mCherry-pA cassette was inserted into pX330 to get the pX330-mcherry as described previously.¹⁸ The single-guide RNAs (sgRNAs) targeting *Tex11* genes were synthesized, annealed, and ligated to the pX330-mcherry plasmid that was digested with *Bbs* I. All the inserted sequences of plasmids were validated by Sanger sequencing. Primers used in this study are listed in **Supplementary Table 1**.

Lipofectamine transfection of SSCs and cell sorting

Before lipofectamine transfection, SSCs were trypsinized, centrifuged, and re-suspended with Opti-MEM (Invitrogen) to a new plate. Thirty minutes later, the Opti-MEM was gently replaced with SSC medium. The pX330-mcherry plasmids harboring the corresponding sgRNAs and oligo DNA were transfected into SSCs with lipofectamine 3000 according to the manufacturer's instruction. Ten hours to 12 h later, the supernatant was aspirated and fresh SSCs were added.

Twenty-four hours after transfection, the SSCs expressing mCherry were sorted with flow cytometry (Beckman Moflo Astrios, Fort Collins, CO, USA), and one mCherry-positive cell was deposited into each well of the 96-well plates. After 3–4 weeks, SSC clones were trypsinized and expanded for genotyping.

Transplantation of SSCs

For SSC transplantation, busulfan (40 mg kg^{-1})-treated 4-week-old *mT/mG* (B6D2F1 background) or 14–21-day-old *Kit^w/Kit^{w/y}* male mice were used as the recipient mice. Approximately 8 μl (2×10^4 cells per μl) of the donor cell suspensions was injected into the seminiferous tubules of an *mT/mG* testis, and 2 μl was introduced into the *Kit^w/Kit^{w/y}* testis through the efferent duct. The mice were sacrificed 2 months later, and the testes were examined for further analysis.

Round spermatid injection (ROSI)

Metaphase II-arrested oocytes were collected from superovulated B6D2F1 females (8–10 weeks) and cumulus cells were removed using hyaluronidase. After decapsulation and digestion, the testicular cell suspensions were filtered through a 40- μm filter (Millipore). Then, the suspensions were suspended with PBS containing 8% FBS. The haploid cells from the testes were sorted according to a reported protocol. First, the cell suspensions were incubated with the Hoechst 33342 (5 $\mu\text{g ml}^{-1}$) at 37°C for 10 min. After washing with PBS/FBS twice, haploid cells were sorted with flow cytometry. The round spermatids were then injected into the oocytes in a droplet of HEPES-CZB medium containing 5 $\mu\text{g ml}^{-1}$ cytochalasin B (CB) using a blunt Piezo-driven pipette. The injected oocytes were activated by treatment with SrCl₂ for 5–6 h and maintained in the potassium simplex optimization medium (KSOM) medium at 37°C under 5% CO₂ in air. Two-cell embryos were transferred into the oviducts of pseudopregnant Institute of Cancer Research (ICR) females. Live fetuses were born on day 19.5 of gestation.

Purification and Sanger sequencing of genomic DNA

Genomic DNA was isolated using the TIANamp Genomic DNA Kit (TIANGEN, Beijing, China), followed by PCR amplification for Sanger sequencing. For blunting cloning sequencing, the targeted sequence was amplified from the genome by high-fidelity DNA polymerase and then purified by the Universal DNA Purification Kit (TIANGEN). The editing efficiency was calculated through blunting cloning (TransGen Biotech, Beijing, China) by picking up more than 20 *Escherichia coli* clones for analysis. Primers used in this study are listed in **Supplementary Table 1**.

Bisulfite sequencing

Bisulfite sequencing was performed using the EZ DNA methylation kit (Zymo Research, Irvine, CA, USA) following the manufacturer's manual. The PCR products were cloned into pMD18T TA cloning vector (Takara, Tokyo, Japan), and individual clones were then sequenced for subsequent analysis. Primers used in this study are listed in **Supplementary Table 1**.

RNA extraction and real-time quantitative PCR

Total RNA was isolated from the cells using TRIzol reagent (Invitrogen). The cDNA was obtained from about 1 μg RNA with reverse transcription reaction by the ReverTra Ace qPCR RT Master Mix (TOYOBO, Osaka, Japan). Real-time quantitative PCR reactions (rtqPCR) were performed on a Bio-Rad CFX96 using the SYBR Green Mix (TOYOBO) in triplicate. All the gene expression levels were normalized to the internal standard gene glyceraldehyde-3-phosphate dehydrogenase (*Gapdh*). Primers used in this study are listed in **Supplementary Table 1**.



Histological and immunostaining analysis

The testis, epididymis, and ovary were fixed in 4% paraformaldehyde overnight at room temperature; dehydrated with different concentration gradients of alcohol; and embedded in paraffin and sectioned. Paraffin sections on slides were dewaxed in xylene and rehydrated in different concentration gradients of alcohol, followed by staining with hematoxylin and eosin.

Library preparation for whole-genome sequencing (WGS)

A total amount of 0.2 µg DNA per sample was used as input material for the DNA library preparations. Sequencing library was generated using NEBNext® Ultra™ DNA Library Prep Kit for Illumina (NEB, Ipswich, MA, USA) following the manufacturer's recommendations, and index codes were added to each sample. Briefly, genomic DNA sample was fragmented by sonication to a size of 350 bp. Then, DNA fragments were end polished, A-tailed, and ligated with the full-length adapter for Illumina sequencing, followed by further PCR amplification. After PCR products were purified by AMPure XP system (Beckman Coulter, Beverly, MA, USA), DNA concentration was measured by Qubit® 3.0 Fluorometer (Invitrogen), and libraries were analyzed for size distribution by NGS3K/Caliper and quantified by real-time PCR (3 nmol l⁻¹).

Library preparation for transcriptome sequencing

A total amount of 1 µg RNA per sample was used as input material for the RNA sample preparations. Sequencing libraries were generated using NEBNext® Ultra™ RNA Library Prep Kit for Illumina® (NEB) following the manufacturer's recommendations, and index codes were added to attribute sequences to each sample.

Briefly, mRNA was purified from total RNA using poly-T-oligo-attached magnetic beads. Fragmentation was carried out using divalent cations under elevated temperature in NEBNext First-Strand Synthesis Reaction Buffer (×5). First-strand cDNA was synthesized using random hexamer primer and M-MuLV Reverse Transcriptase (RNase H⁻). Second-strand cDNA synthesis was subsequently performed using DNA polymerase I and RNase H. The remaining overhangs were converted into blunt ends via exonuclease/polymerase activities. After adenylation of 3' ends of DNA fragments, NEBNext Adaptor with hairpin loop structure was ligated to prepare for hybridization. In order to select cDNA fragments of preferentially 250–300 bp in length, the library fragments were purified with AMPure XP system (Beckman Coulter, Brea, CA, USA). Then, 3 µl USER Enzyme (NEB) was used with size-selected, adaptor-ligated cDNA at 37°C for 15 min followed by 5 min at 95°C before PCR. Then, PCR was performed with Phusion High-Fidelity DNA polymerase, Universal PCR primers, and Index (X) Primer. At last, PCR products were purified and library quality was assessed on the Agilent Bioanalyzer 2100 system.

WGS data analysis

Raw reads were filtered by fastp (version 0.20.0) to acquire clean reads, and then mapped to mouse genome (mm10) using BWA tool with default parameters. For single-nucleotide polymorphism (SNP) and Indel calling, data preparation was executed according to the GATK best practices with GATK version 4.1.5.0, and well-prepared bam files were subjected to Mutect2 for SNP calling. Then, the resultant SNPs were filtered by hard filters with parameters, namely DP <10, QD <2.0, QUAL <30.0, SOR >3.0, FS >60.0, Q <40.0, MQRankSum <-12.5, and ReadPosRankSum <-8.0. Indels were filtered with parameters such as DP <10, QD <2.0, QUAL <30.0, ReadPosRankSum <-20.0, and FS >200.0. Passed SNPs and Indels were filtered by allele DP >10,

minor allele frequency >0.35 for heterozygous SNPs, allele frequency >0.85 for homozygous SNPs. All SNPs and Indels were annotated by ANNOVAR (October 24, 2019). All primers used to confirm called SNPs and Indels are generated by Primer3 program. All predicted off-target sites were calculated by Cas-OFFinder (mouse genome: mm10) with at most five mismatches. And overlapped all called SNPs within predicted off-target sites (within ±20 bp) using Excel. The top predicted sites were examined by PCR (primers used were generated by Primer3) and sequencing.

Production of Cas9 mRNA and sgRNAs

First, pX330 plasmid including T7 promoter was linearized by *Not* I. The linearized templates were purified and *in vitro* transcribed with mMESSAGE mMACHINE T7 ULTRA kit (Life Technologies, Carlsbad, CA, USA). SgRNAs with T7 promoter were amplified by PCR and *in vitro* transcribed using MEGAshortscript™ T7 kit (Life Technologies). After transcription, the Cas9 mRNA and the sgRNAs were purified with MEGAclean™ kit (Life Technologies) according to the manufacturer's instructions.

Zygote injection

C57BL/6 female mice were superovulated and mated with the male C57BL/6 mice. For embryo injection, donor oligo (100 ng µl⁻¹) was mixed with Cas9 mRNAs (100 ng µl⁻¹) and sgRNA (50 ng µl⁻¹) and injected into the embryos. The injected embryos were cultured in KSOM until 2-cell embryonic stage and transferred into pseudopregnant female mice.

The sequences of injected sgRNA were as follows: AATATGCTGATGCCCTACAC, oligo donor: GTGAAT TTTGGAAAAATCTATGACTTTGTTGTTTTTTTTTAACTTTA GGTCCAAAAATATGCTTTGGTACCCTACACTGGTACAGTTAT TCTCTGAAGTTGTATGAGTATGATAAAGCAGATCTGGATT.

Material availability

Plasmids and mouse strains generated in this study are available from the Lead Contact.

Data accession

The raw data of RNA-seq and processed data of bulk RNA-seq and WGBS in this study were deposited at Gene Expression Omnibus (GEO) with accession numbers GSE158977, 158978, and 158979.

RESULTS**Male mice carrying an azoospermia patient-originated TEX11 mutation display meiotic arrest**

TEX11 mutations have been identified in patients with azoospermia^{9,10,22} recently. To test the PDMX model, we chose a frame shift mutation in exon 16 (1258Ins [TT]) revealed in an azoospermic family.¹⁰ This mutation results in a stop codon at the 431st amino acid (Supplementary Figure 1a), leading to a truncated protein TEX11 without the final 948 amino acids. Histological analysis of the patient's testis biopsy indicated meiotic arrest at the pachytene stage,¹⁰ suggesting the possibility of existing SSCs in the testes. We first introduced the patient-derived mutation into the mouse genome through co-injection of Cas9 mRNA, sgRNA targeting exon 16, and exogenous single-stranded DNA oligo carrying the mutation into zygotes (C57BL/6 background) according to a previous report¹⁸ (Supplementary Figure 1b). Of 150 injected zygotes, a total of 31 live pups were born (Supplementary Table 2). DNA sequencing analysis revealed that six of them were carrying knockin mutation at the targeted site in exon 16 (Supplementary Figure 1c), which were

used as founders for further analysis. All founders displayed normal development. However, after long-term breeding of founders with wild-type mice, males failed to give rise to any births, while female heterozygous-mutant founders displayed reproductive ability and could have progeny normally. We dissected ovaries and testes from founders and observed a similar size in mutant ovary but significant smaller size in mutant testes (**Supplementary Figure 1d** and **1f**). Histological analysis indicated normal gametogenesis in mutant ovary (**Supplementary Figure 1e**) but meiotic arrest in mutant testis and no sperm in epididymis (**Supplementary Figure 1g**). These results recapitulate the observations in azoospermic family, in which the patient carried *TEX11* mutation inherited from his heterozygous-mutated mother.¹⁰

We thus set up a breeding system to obtain *Tex11*-mutant males (hereafter *Tex11*^{PM/Y}) for further analysis through using female *Tex11*^{PM/X} individuals backcrossed with wild-type males. As expected, male offspring carrying mutant *Tex11* normally grew up to adult but displayed sterility (**Supplementary Figure 2a**). The weights of the mutant testes were significantly lighter than that of wild-type controls (**Figure 1a** and **1b**). Histological analysis of testes from adult *Tex11*^{PM/Y} mice showed that *Tex11* mutation causes spermatogenic failure, leading to rare germ cells in *Tex11*^{PM/Y} seminiferous tubules and epididymis (**Supplementary Figure 2b** and **2c**). To check the effect of *Tex11* mutation on SSCs, we analyzed the expression of promyelocytic leukemia zinc finger (PLZF), the specific marker of SSCs²⁵ in juvenile testes. The results showed comparable SSC populations in *Tex11*^{PM/Y} to littermate controls (**Figure 1c** and **1d**), suggesting that *TEX11* is not required for the maintenance of undifferentiated spermatogonia.

Previous studies have shown that *Tex11*^{-/-} exhibited defects in chromosomal synapsis.^{23,24} We thus performed the co-immunostaining of spermatocyte spreads prepared from *Tex11*^{PM/Y} for mutl homolog 1 (*MLH1*, crossover marker) and synaptonemal complex protein 3 (*SCP3*, synaptonemal complex marker). The results indicated that patient-derived mutation caused aberrant chromosomal synapsis in mouse testes (**Figure 1e** and **1f**). Terminal deoxynucleotidyl transferase biotin-dUTP nick end labeling (TUNEL) analysis showed that apoptosis increased dramatically in *Tex11*^{PM/Y} seminiferous epithelium (**Figure 1g** and **1h**), especially in cells at stages of IV and XII (**Supplementary Figure 2d** and **2e**), consistent with previous observations about increased apoptosis in *Tex11*^{-/-} testes.²⁴ Taken together, these data show that patient-derived *TEX11* mutation disrupts chromosomal synapsis, leading to meiotic arrest, followed by spermatocyte apoptosis in mouse seminiferous tubules, which resembles the phenotypes observed in patients with azoospermia.⁹

SSCs isolated from *Tex11*^{PM/Y} mice are normal

Having demonstrated that SSCs were unaffected in the testes of mutant males, we next attempted to derive SSC lines from newborn *Tex11*^{PM/Y} males according to well-established protocols.^{21,26–28} Briefly, CD146-positive cells were enriched from testicular cells dissociated from mutant testes and cultured in a standard SSC culture medium²⁹ (**Figure 2a** and **2b**), leading to a stable SSC line carrying *Tex11*^{PM/Y} (**Figure 2c**). The mutant SSCs showed typical SSC morphology, normal proliferation, and expression of SSC markers at similar levels as wild-type SSCs (**Figure 2d–2f**). Next, we compared the whole-gene expression of *Tex11*^{PM/Y} SSCs with those of normal SSCs by performing

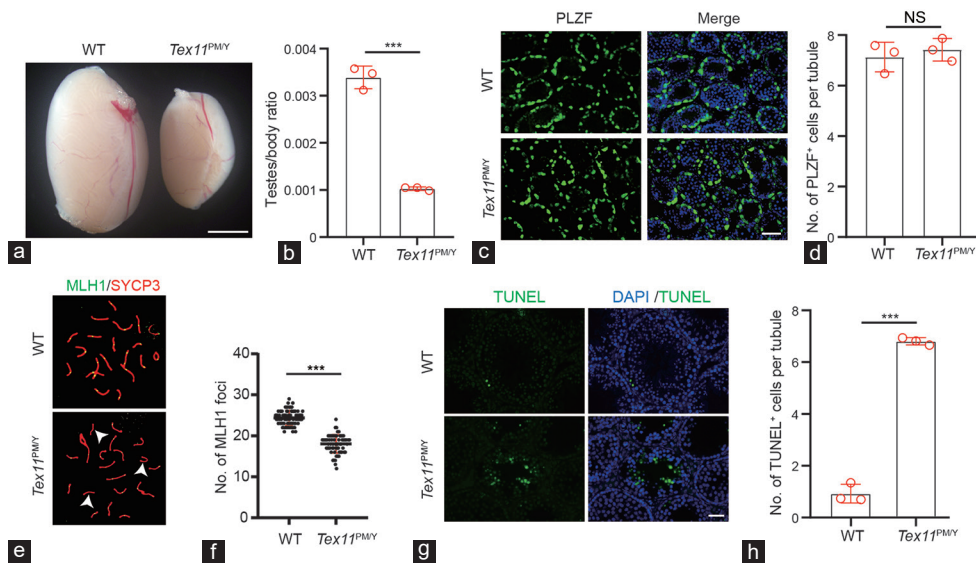


Figure 1: Male mice carrying an azoospermia patient-derived *TEX11* mutation display meiotic arrest. **(a)** Testis morphology of WT and *Tex11*^{PM/Y} mice. Scale bar = 100 mm. **(b)** Relative testis/body weight of WT and *Tex11*^{PM/Y} mice. The average values of three separate experiments are plotted. Error bar: s.d. Significance was determined by two-tailed, unpaired Student's *t*-test. **(c)** Immunostaining of 10 dpp testis sections with an anti-PLZF antibody. Green: PLZF; Blue: Hoechst 33342. Scale bar = 50 μ m. **(d)** Quantification of PLZF⁺ cells in 10 dpp testis sections. A total of 237 and 222 tubules from three WT and *Tex11*^{PM/Y} mice were scored. Error bar: s.d. Significance was determined by two-tailed, unpaired Student's *t*-test. NS: no significance. **(e)** Immunostaining of MLH1/SCP3 in spermatocyte spreads prepared from 8-week-old WT and *Tex11*^{PM/Y} mice. Green: MLH1; red: SYCP3. Note the absence of MLH1 foci on three synapsed chromosomes (arrowhead) in the *Tex11*^{PM/Y} sample shown in the bottom image. **(f)** Number of MLH1 foci in *Tex11*^{PM/Y} and WT spermatogonia. A dramatic reduction in the number of MLH1 foci (green) in *Tex11*^{PM/Y} spermatogonia (approximately 15 foci per cell) relative to WT (22 foci per cell). Error bar: s.d. Significance was determined by two-tailed, unpaired Student's *t*-test; ****P* < 0.001. **(g)** TUNEL analysis of *Tex11*^{PM/Y} and WT testis. Massive apoptosis (green) shown in *Tex11*^{PM/Y} tubules. Scale bar = 100 μ m. **(h)** Analysis of apoptotic cells in *Tex11*^{PM/Y} and WT testis. The average values of three separate experiments are plotted. Error bar: s.d. Significance was determined by two-tailed, unpaired Student's *t*-test; ****P* < 0.001. *TEX11*: testis-expressed 11; WT: wild-type; PLZF: promyelocytic leukemia zinc finger; MLH1: mutl homolog 1; SYCP3: synaptonemal complex protein 3; TUNEL: terminal deoxynucleotidyl transferase biotin-dUTP nick end labeling; DAPI: 4',6-diamidino-2-phenylindole; s.d.: standard deviation; dpp: days postpartum.

RNA sequencing (RNA-seq). A similar expression pattern was observed for global genes in both cells (**Figure 2g** and **Supplementary Figure 3a**). Further analysis showed an unaffected transcriptional level among SSC self-renewal, meiotic, and imprinted genes upon *Tex11* mutation (**Figure 2h**, **Supplementary Figure 3b** and **3c**). Only two genes, including *Tex11*, were found to be differentially expressed between WT and *Tex11^{PM/Y}* samples, suggesting a highly similar expression pattern (**Supplementary Figure 3d** and **3e**). Taken together, these results indicated that *Tex11^{PM/Y}* SSCs are generally normal, implying that these cells after genetic correction may resume spermatogenesis.

Gene therapy in *Tex11^{PM/Y}* SSCs

To correct the mutation, we designed two sgRNAs targeting upstream and downstream of the mutant site (termed sgRNA-1 and sgRNA-2, respectively) and transfected pX330-mCherry plasmids¹⁸

expressing Cas9 and sgRNA-1 or sgRNA-2 and exogenous plasmid carrying wild-type sequence into *Tex11^{PM/Y}* SSCs (**Figure 3a**). One day later, the SSCs expressing mCherry were enriched, in which the CRISPR-Cas9 system was successfully transfected, and single mCherry-positive SSCs were deposited into each well of the 96-well plates (**Supplementary Figure 4a** and **4b**) according to a previously reported protocol.²⁹ From a total of 580 single SSCs for each sgRNA, we established 17 and 16 clonal SSC lines for sgRNA-1 and sgRNA-2, respectively (**Supplementary Table 3**). Further analysis showed that sgRNA-1 efficiently targeted the mutant *Tex11* and led to HDR-mediated repair of the *Tex11* gene in three SSC lines (**Figure 3c**). By contrast, no HDR-based repair was detected in SSC clones transfected with sgRNA-2 (**Supplementary Figure 4c** and **Supplementary Table 3**).

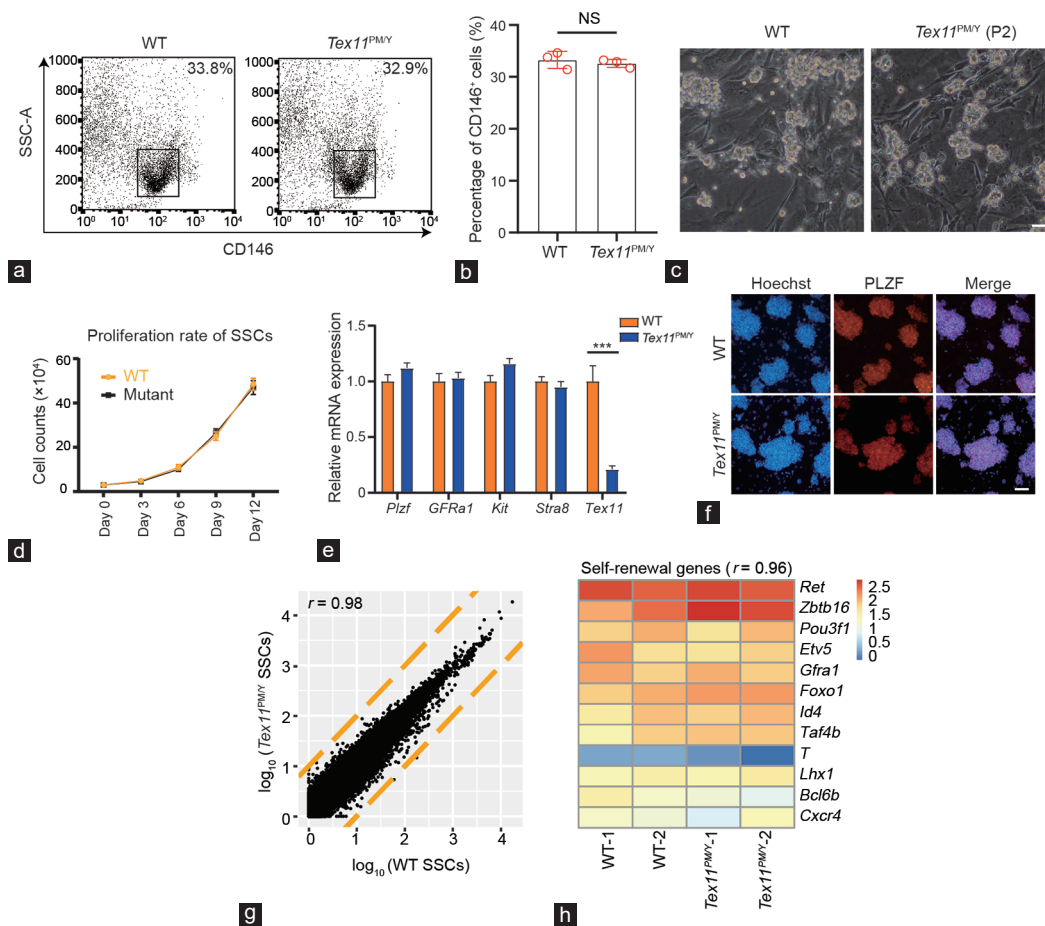


Figure 2: SSCs isolated from *Tex11^{PM/Y}* mice are normal. **(a)** Flow cytometric analysis of the ratio of SSCs using CD146 antibody in 10-day-old WT and *Tex11^{PM/Y}* testicular cells. Small black boxes represent the positive population of SSCs. **(b)** The ratio of CD146-positive cells in WT and *Tex11^{PM/Y}* testicular cells (three mice per group) was scored. Error bar: s.d. Significance was determined by two-tailed, unpaired Student's *t*-test; NS: no significance. **(c)** Morphology of cultured WT and *Tex11^{PM/Y}* SSCs. P2: passage 2. Scale bar = 100 μ m. **(d)** Proliferation rate of WT and *Tex11^{PM/Y}* SSCs during *in vitro* culture. The average values of three separate experiments are plotted. Error bar: s.d. Significance was determined by two-tailed, unpaired Student's *t*-test. **(e)** Expression of marker genes in WT and *Tex11^{PM/Y}* SSCs. *Id4* and *Sohlh2* were used as undifferentiated marker genes, while *Kit* and *Stra8* were used as differentiated marker genes. The average values of three separate experiments are plotted; error bar: s.d. Significance was determined by two-tailed, unpaired Student's *t*-test; ****P* < 0.001. **(f)** Immunostaining of PLZF in WT and *Tex11^{PM/Y}* SSCs. Scale bar = 200 μ m. **(g)** Scatter plot of \log_{10} -transformed average gene expression profiles. Global gene expression profiles of WT and *Tex11^{PM/Y}* SSCs were obtained from RNA-seq analysis (*r* is the Pearson's correlation coefficient; yellow lines indicate two-fold upregulation and downregulation). **(h)** Heatmap correlation of SSC self-renewal genes in WT and *Tex11^{PM/Y}* SSCs (*r* is the Pearson's correlation coefficient). WT: wild-type; *Tex11*: testis-expressed 11; SSCs: spermatogonial stem cells; s.d.: standard deviation; PLZF: promyelocytic leukemia zinc finger; SSC-A: Side Scatter-area; *Id4*: inhibitor of DNA binding 4; *Sohlh2*: spermatogenesis and oogenesis specific basic helix-loop-helix 2; *Kit*: Kit proto-oncogene; *Stra8*: stimulated by retinoic acid 8; *Ret*: ret proto-oncogene; *Zbtb16*: zinc finger and BTB domain containing 16; *Pou3f1*: POU class 5 homeobox 1; *Etv5*: ETS variant transcription factor 5; *Gfra1*: GDNF family receptor alpha 1; *Foxo1*: forkhead box O1; *Taf4b*: TATA-box binding protein associated factor 4b; *T*: brachyury; *Lhx1*: LIM homeobox 1; *Bcl6b*: BCL6B transcription repressor; *Cxcr4*: C-X-C motif chemokine receptor 4.

Three repaired SSC lines (termed HDR-1, 2, and 3) derived from single SSC expansion after CRISPR-Cas9-mediated HDR correction of the patient-derived mutation in *Tex11* gene restored the expression of *Text11* to the level similar to that of wild-type SSCs (Figure 3d). These SSCs proliferated *in vitro* normally, showed typical SSC morphology, and expressed SSC marker genes (Figure 3b, Supplementary Figure 5a and 5b). To further assess epigenetic inheritance, we performed bisulfite sequencing of two paternally imprinted regions, H19 imprinted maternally expressed transcript (*H19*)-DMR and intergenic differentially methylated region (*IG*)-DMR, and one maternally imprinted region, small nuclear ribonucleoprotein polypeptide N (*Snrpn*)-DMR in mutant and wild-type SSCs, and confirmed that both cell lines stably sustained typical paternally imprinted state (Figure 3e). One major challenge of CRISPR-Cas9-based therapeutic application is the occurrence of unintended off-target mutation at certain genome site depending on the specificity of the chosen sgRNA and intrinsic properties of Cas9. This becomes even more serious when germ cells are the target cells for gene therapy, because the unwanted modifications produced in the germ cells will pass on to the offspring genome, which might not only give rise to other genetic diseases in current individuals but also will pass on to next generations.^{30–34} To evaluate the risk of our therapy, we analyzed off-target effects in the three SSC lines derived from single SSCs that harbor corrected *Tex11*. We first searched all possible off-target sites with at most five mismatches for the sgRNA-1 against the whole mouse genome using Cas-OFFinder³⁵ and found a total of 1166 possible off-target sites with no sites that show 0/1/2 mismatches, which indicates that the specificity of our sgRNA is sufficient. We then amplified and sequenced all possible sites within three mismatches but found that

none of the sites were affected by our method (Supplementary Table 4). Next, to dive in the specificity of our method, we analyzed the genomic mutation between one cured SSC line (HDR-1) and its parental *Tex11*^{PM/Y} SSCs using WGS (×40; Supplementary Table 5). The results indicated normal karyotype features and no significant genome copy number variations in both SSCs (Supplementary Figure 6a). We found no *Tex11* mutation in the HDR-1 genome sites, confirming that HDR-1 SSC line was derived from a single cell (Supplementary Figure 6b). Thirty-six single-nucleotide variations (SNVs) and six indels were called using Mutect2 (GATK toolkit) between *Tex11*^{PM/Y} SSCs and corrected HDR-1 SSCs (Supplementary Table 6). At the time point of performing WGS, both cell lines have already passaged eight times, individually, leading to an average four SNVs or indels per cell division *in vitro*, with the mutation rate in our system being comparable with that of spontaneous mutation rate (4–5 per cell division) *in vivo*.³⁶ None of these SNVs or indels were annotated within the exonic gene region (Supplementary Table 6). Among all the detected SNVs and indels between those two cell lines, none of the mutations resided on any of the predicted off-target sites. Taken together, these results demonstrate that CRISPR-Cas9-mediated gene correction in *Tex11*^{PM/Y} SSCs does not induce obvious off-target effects in SSCs, consistent with our previous observations in gene-treated SSCs carrying a disease-causing homozygous mutation.²¹

Corrected SSCs restore spermatogenesis in the testes of infertility models

Finally, we investigated whether SSCs with corrected *Tex11* could restore spermatogenesis *in vivo*. To this end, we first transplanted HDR-1 SSCs into the testis of *Tex11*^{PM/Y} mice

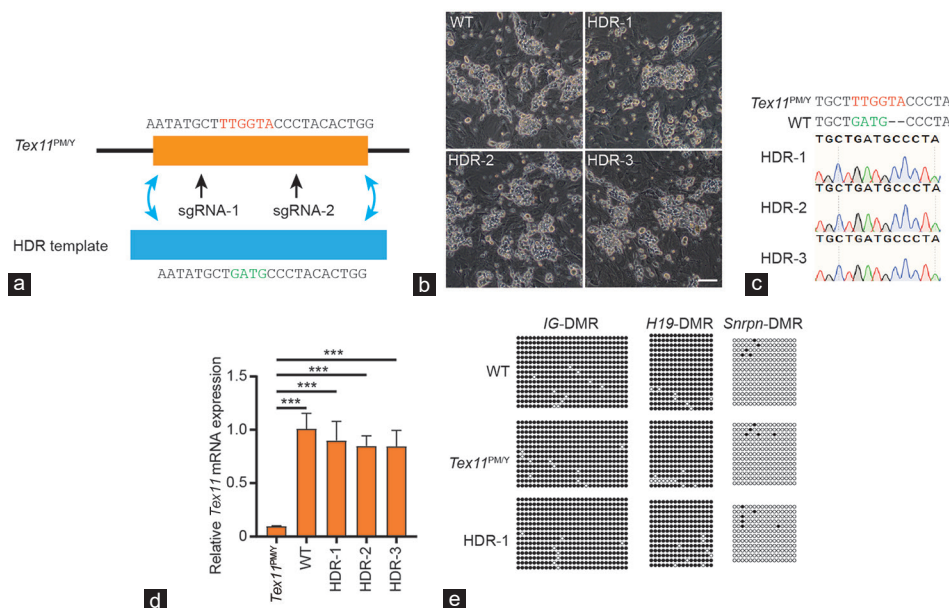


Figure 3: Correction of *Tex11* mutation via CRISPR-Cas9-mediated gene editing in SSCs. (a) Schematic for *Tex11* gene correction via HDR induced by CRISPR-Cas9 system and HDR template with WT sequence of *Tex11*. The mutant nucleotides were marked in red, while the WT nucleotides were in green. (b) Morphology of the three established SSC lines with correct *Tex11* sequence (termed HDR-1, 2, and 3). Scale bar = 100 μm. (c) DNA sequencing analysis of SSCs from HDR-1/2/3. Note that the sequences of PCR products amplified from the *Tex11* gene show that HDR-1/2/3 carry corrected *Tex11* gene. (d) Transcriptional analysis of *Tex11* in the corrected SSCs lines. The expression values were normalized to that of WT. The average values of three separate experiments are plotted; error bar: s.d. Significance was determined by two-tailed, unpaired Student's *t*-test; ****P* < 0.001. (e) DNA methylation analysis of the DMRs of *H19*, *IG*, and *Snrpn* in *Tex11*^{PM/Y} and HDR-1 SSCs. Open, filled, and gray circles represent unmethylated, methylated, and uncertain CpG sites, respectively. WT: wild-type; *Tex11*: testis expressed 11; SSCs: spermatogonial stem cells; s.d.: standard deviation; sgRNA: single-guide RNA; CRISPR-Cas9: clustered regularly interspaced short palindromic repeats-CRISPR-associated endonuclease 9; DMR: differentially methylated regions; *H19*: H19 imprinted maternally expressed transcript; *IG*: intergenic differentially methylated region; *Snrpn*: small nuclear ribonucleoprotein polypeptide N; CpG: cytosine-guanine; HDR: homology-directed repair.

to mimic autotransplantation situation in patient treatment (**Supplementary Figure 7a**). However, no spermatogenesis occurred in all the three tested recipient mice (**Supplementary Figure 7b and 7c**), indicating that cured SSCs cannot find the niches when normal *Tex11^{PM/γ}* SSCs exist in seminiferous tubules. We then attempted to test the ability of the spermatogenesis of cured SSCs by transplantation of HDR-1 SSCs and *Tex11^{PM/γ}* SSCs as control into the recipient testis of *Kit^W/Kit^{WV}* (*C-Kit* double heterozygotes) males, a well-established infertility model³⁷ or busulfan-treated *mT/mG* males expressing membrane-targeted tdTomato³⁸ (**Figure 4a** and **Supplementary Figure 8a**). Two months after the transplantation, we observed significantly increased size of testes with transferred HDR-1 SSCs compared to that of control transplanted testes with *Tex11^{PM/γ}* SSCs (**Figure 4b** and **4c**). Histological analyses indicated that HDR-1 SSCs successfully migrated toward germline niches, recolonized the seminiferous tubules, and restored the spermatogenesis of infertile testes³⁹ (**Figure 4d** and **4e**). Finally, haploid spermatids could be enriched and used for intracytoplasmic round spermatid injection (ROSI; **Figure 4f** and **4g**, and **Supplementary Figure 8b**). The injected oocytes efficiently developed into two-cell embryos, which were then transplanted into the recipient oviducts of

pseudopregnant females. We obtained a total of 61 pups on 19.5 days of gestation, at a rate of 16.1% of transferred embryos, similar to that of ROSI with wild-type round spermatids (**Figure 4h** and **Table 1**). Genotyping analysis indicated that all of them carry wild-type *Tex11* (**Supplementary Figure 9a**). As the resultant pups were derived from a cured SSC line (HDR-1) that carried SNPs detected by WGS, we thus used these SNPs as molecular markers to further demonstrate their paternal origin. As expected, the analysis of five SNPs indicated that two tested pups were originated from HDR-1 (**Supplementary Figure 9b** and **Supplementary Table 7**). The pups grew to adulthood and males could give rise to progeny normally, demonstrating the successful transmission of corrected *Tex11* in HDR-1 to next generations (**Supplementary Table 8**).

DISCUSSION

We have demonstrated the feasibility of infertility treatment by correcting a genetic defect causing azoospermia through a combination of *in vitro* expansion of SSCs and CRISPR-Cas9-based gene therapy (**Figure 5**). This PDMX pipeline involved validating the monogenic mutation that causes azoospermia through generation of mouse models by introduction of disease-related *TEX11* mutation into mouse genome that recapitulates the phenotype of meiotic arrest. SSCs were isolated

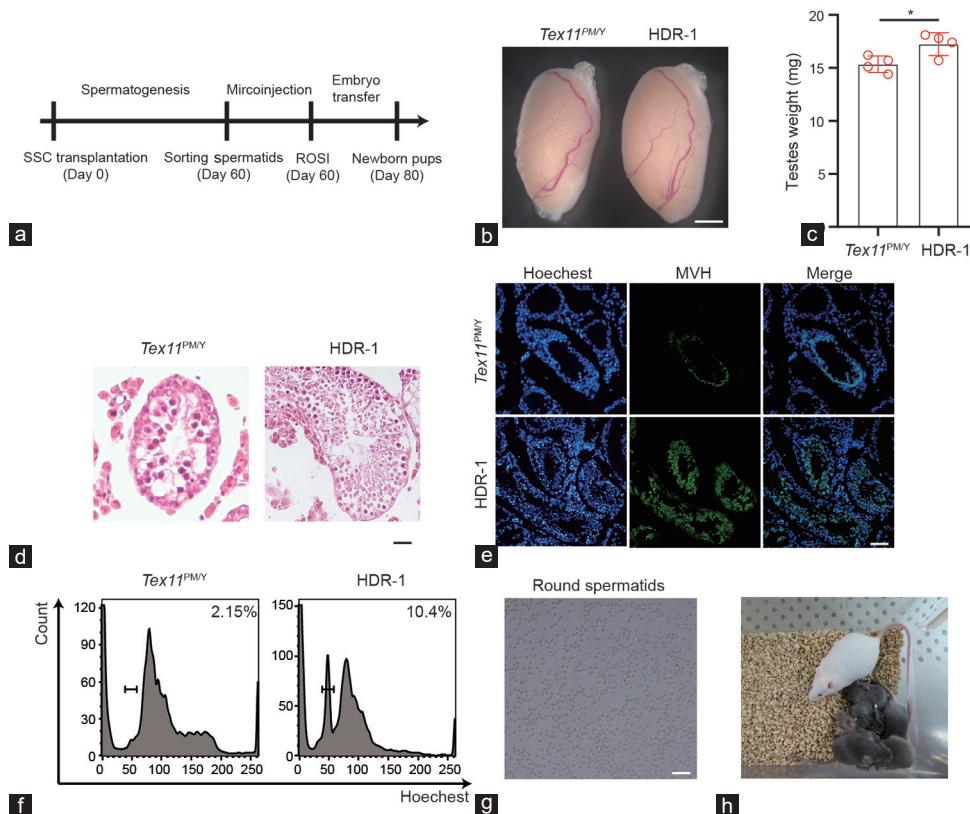


Figure 4: Corrected SSCs restore spermatogenesis in the testes of *Kit^W/Kit^{WV}* mice. **(a)** Diagram showing the repaired SSCs derived from single SSCs without off-target mutations which are selected for transplantation into infertile *Kit^W/Kit^{WV}* male mice. Two months later, spermatids are isolated from reconstituted testes and injected into mature oocytes to produce healthy mice carrying corrected *Tex11* gene. **(b)** Testis morphology of *Tex11^{PM/γ}* and HDR-1 SSC-transplanted *Kit^W/Kit^{WV}* mice. Scale bar = 100 mm. **(c)** Weight of *Tex11^{PM/γ}* and HDR-1 SSC-transplanted *Kit^W/Kit^{WV}* testes. The average values of three separate experiments are plotted. Error bar: s.d. Significance was determined by two-tailed, unpaired Student's *t*-test; **P* < 0.05. **(d)** Histological analyses of the *Tex11^{PM/γ}* and HDR-1 SSC-transplanted *Kit^W/Kit^{WV}* testis. Note successful spermatogenesis in the HDR-1 SSC-transplanted testis. Scale bar = 40 μm. **(e)** Immunostaining of MVH in *Tex11^{PM/γ}* and HDR-1-transplanted *Kit^W/Kit^{WV}* testis. Green: MVH; blue: Hoechst. Scale bar = 100 μm. **(f)** Round spermatids are sorted from testicular cells of reconstituted testes according to DNA content. **(g)** Morphology of round sperm sorted from HDR-1-transplanted testis. Scale bar = 50 μm. **(h)** Pups (black coat color) on 12 dpp developed from transferred two-cell embryos generated after the injection of round spermatids from HDR-1 SSCs into mature oocytes. WT: wild-type; *Tex11*: testis expressed 11; SSCs: spermatogonial stem cells; ROSI: round spermatid injection; s.d.: standard deviation; HDR: homology-directed repair; dpp: days postpartum.

from *Tex11^{PMY}* mice and expanded *in vitro*. CRISPR-Cas9-induced HDR was used to correct the gene defect in SSCs, and SSC lines were established through single-cell expansion. Genotyping, methylation, and off-target analyses enabled the selection of SSCs with the desired genotype, with normal imprinted state, and without off-target mutations for further implementation. To assess whether the genetic correction restored spermatogenesis, we transplanted cured SSCs into the recipient testes of two infertility models. The spermatogenesis was resumed in the seminiferous tubules of these animals, as demonstrated by the enrichment of haploid spermatids 2 months after SSC transplantation. As expected, round spermatids, through ROSI, gave rise to offspring normally. Importantly, the resultant males exhibited normal fertility, indicating the transmission of the corrected gene to

next generations. Thus, CRISPR-Cas9-mediated gene therapy in SSCs corrected the genetic defect causing azoospermia.

A critical step of PDMX is the isolation and expansion *in vitro* of SSCs from infertility individuals. Mouse and rat SSCs can be maintained in long-term culture and still possess the potential to colonize and initiate spermatogenesis in seminiferous tubules when transplanted into the testes of infertility recipients.¹⁶ Strikingly, mouse SSCs that were cultured *in vitro* over 2 years generally sustain normal genetic and epigenetic stability and could be used to produce spermatogenesis and fertile offspring after transplantation.⁴⁰ Moreover, mouse SSCs after 14-year cryopreservation could still reconstitute the spermatogenesis in the recipient testes.⁴¹ These observations imply that SSCs are a promising cell resource for stem

Table 1: Mice produced through injection of round spermatids derived from transplanted spermatogonial stem cells into mature oocytes

Round spermatid source	Recipient mice for SSC transplantation	Types of transplanted SSCs	Genetic background of SSCs	Number of injected oocytes	Number of transferred two-cell embryos	Number of live-born pup, n (%)	Number of pups with corrected <i>Tex11</i>
Recipient mice	<i>Kit^{WJ}Kit^{WV}</i>	HDR-1	C57×DBA	161	134	21 (15.67)	20
Recipient mice	<i>Kit^{WJ}Kit^{WV}</i>	<i>Tex11^{PMY}</i>	C57×DBA	155	36	0 (0)	0
Recipient mice	Busulfan-treated <i>mT/mG</i>	HDR-1	C57×DBA	140	120	22 (18.33)	22
Recipient mice	Busulfan-treated <i>mT/mG</i>	HDR-1	C57×DBA	145	124	18 (14.51)	18
Control	-	-	-	150	130	24 (18.46)	0

Tex11: testis-expressed 11; SSCs: spermatogonial stem cells; HDR: homology-directed repair; DBA: Dilute Brown Non-Agouti

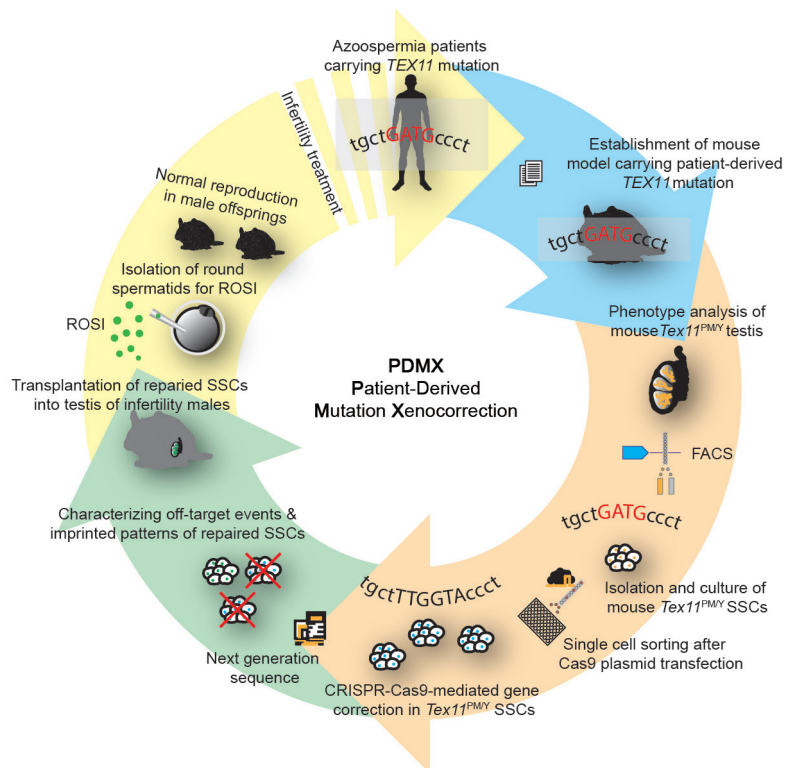


Figure 5: Scheme for PDMX model of male azoospermia therapy. *TEX11* mutation has been identified in patients with azoospermia. To validate its pathogenic roles, mouse model with the patient-derived mutation (*Tex11^{PMY}* mice) was derived, which recapitulated patient's pathological phenotypes and displayed meiotic arrest. SSCs isolated from the testis of the *Tex11^{PMY}* mice were expanded *in vitro*. CRISPR-Cas9-mediated gene correction was employed in *Tex11^{PMY}* SSCs and repaired SSC lines were derived through single SSC expansion, followed by whole-genome sequencing to exclude the off-target mutations. The repaired SSCs were then used for transplantation to restore spermatogenesis in infertility males. PDMX model thus provides proof-of-principle evidence for curing human azoospermia carrying a single mutation that causes meiotic arrest. *TEX11*: testis-expressed 11; SSCs: spermatogonial stem cells; ROSI: round spermatid injection; CRISPR-Cas9: clustered regularly interspaced short palindromic repeats-CRISPR-associated endonuclease 9; PDMX: patient-derived mutation xenocorrection.

cell therapies with regard to male infertility.² However, while several independent groups reported the *in vitro* culturing of human SSCs using different protocols, a standard protocol that can be replicated by different groups is still an unmet need.⁴² Furthermore, transplantation of SSCs to regenerate spermatogenesis, the golden standard assay for SSC functional analysis, needs to be established in humans. Interestingly, the failed spermatogenesis after autotransplantation into meiotic arrest males in this study suggests that it is critical to remove uncorrected SSCs before transplantation of cured SSCs into patient testes, or it may be necessary to establish a protocol of *de novo* morphogenesis of testis in humans.²⁸ Therefore, a future task is to define appropriate culture conditions that would enable efficient establishment of human SSC lines from seminiferous tubule biopsy samples, which would facilitate the potential applications of these cells in stem cell therapies.

Another critical step of our PDMX model is to identify azoospermia-causing mutations. With the rapid development of high-throughput genome sequencing technologies and bioinformatics methodologies, increasing spermatogenic failure-related mutations are emerging,¹ which can be potentially used as targets for gene therapy to treat male infertility. Thus, we first need to validate that the identified mutations can cause azoospermia indeed. The most stringent strategy of validation is to recapitulate the patients' phenotypes in model organisms, especially in mouse, as demonstrated in this study. Moreover, PDMX model in this study excluded the possibility that the *TEX11* mutation disturbs the self-renewing and proliferating abilities of SSCs, thus enabling the stem cell-based gene therapy.

In summary, we have demonstrated that combined application of SSC *in vitro* expansion and CRISPR-Cas9-mediated gene therapy can be used to cure a genetic disease of male infertility in mice, providing proof-of-principle approach for the treatment of human azoospermia caused by single-gene mutation-induced meiotic arrest.

AUTHOR CONTRIBUTIONS

YHW, MHT, and JSL designed the study. XYL performed mouse embryo microinjection and embryo transplantation. YHW and YFD performed SSC transplantation. YHW performed *in vitro* culture and gene editing of SSCs; YHW and CPL performed genotyping and gene expression experiments. XZ performed TUNEL analysis and meiotic-related gene immunofluorescence. MY analyzed the whole-exome sequencing and RNA-seq data. YHW and JSL wrote the manuscript. All authors read and approved the final manuscript.

COMPETING INTERESTS

All authors declare no competing interests.

ACKNOWLEDGMENTS

This study was supported by Genome Tagging Project and grants from the Chinese Academy of Sciences, the National Key Research and Development Program of China, Shanghai Municipal Commission for Science and Technology, and the National Natural Science Foundation of China (XDB19010204, 2019YFA0109900, OYZDJ-SSW-SMC023, Facility-based Open Research Program, 19411951800, 17JC1420102, 31821004, 32030029, 31730062, 31530048, and 81672117). The research is partly supported by the Fountain-Valley Life Sciences Fund of University of Chinese Academy of Sciences Education Foundation.

Supplementary Information is linked to the online version of the paper on the *Asian Journal of Andrology* website.

REFERENCES

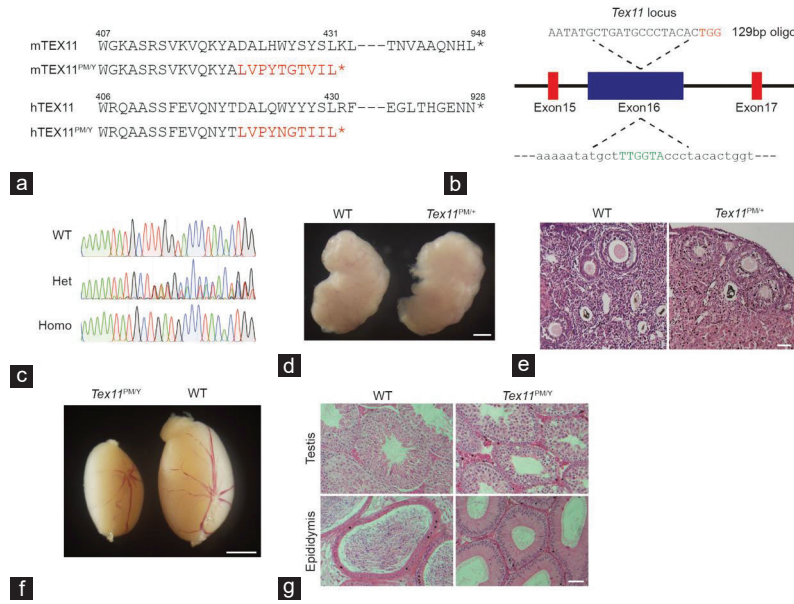
- Krausz C, Riera-Escamilla A. Genetics of male infertility. *Nat Rev Urol* 2018; 15: 369–84.
- Gassei K, Orwig KE. Experimental methods to preserve male fertility and treat male factor infertility. *Fertil Steril* 2016; 105: 256–66.
- Esteves SC. Clinical management of infertile men with nonobstructive azoospermia. *Asian J Androl* 2015; 17: 459–70.
- Tournaye H, Krausz C, Oates RD. Novel concepts in the aetiology of male reproductive impairment. *Lancet Diabetes Endocrinol* 2017; 5: 544–53.
- Tuttelmann F, Ruckert C, Ropke A. Disorders of spermatogenesis: perspectives for novel genetic diagnostics after 20 years of unchanged routine. *Med Genet* 2018; 30: 12–20.
- Riera-Escamilla A, Enguita-Marruedo A, Moreno-Mendoza D, Chianese C, Sleddens-Linkels E, *et al*. Sequencing of a 'mouse azoospermia' gene panel in azoospermic men: identification of *RNF212* and *STAG3* mutations as novel genetic causes of meiotic arrest. *Hum Reprod* 2019; 34: 978–88.
- van der Bijl N, Ropke A, Biswas U, Woste M, Jessberger R, *et al*. Mutations in the stromal antigen 3 (*STAG3*) gene cause male infertility due to meiotic arrest. *Hum Reprod* 2019; 34: 2112–9.
- Yang Y, Guo J, Dai L, Zhu Y, Hu H, *et al*. *XRCC2* mutation causes meiotic arrest, azoospermia and infertility. *J Med Genet* 2018; 55: 628–36.
- Yatsenko AN, Georgiadis AP, Ropke A, Berman AJ, Jaffe T, *et al*. X-linked *TEX11* mutations, meiotic arrest, and azoospermia in infertile men. *N Engl J Med* 2015; 372: 2097–107.
- Yang F, Silber S, Leu NA, Oates RD, Marszalek JD, *et al*. *TEX11* is mutated in infertile men with azoospermia and regulates genome-wide recombination rates in mouse. *EMBO Mol Med* 2015; 7: 1198–210.
- Ben Khelifa M, Ghieh F, Boudjenah R, Hue C, Fauvert D, *et al*. A *MEI1* homozygous missense mutation associated with meiotic arrest in a consanguineous family. *Hum Reprod* 2018; 33: 1034–7.
- Gershoni M, Hauser R, Barda S, Lehavi O, Arama E, *et al*. A new *MEI0B* mutation is a recurrent cause for azoospermia and testicular meiotic arrest. *Hum Reprod* 2019; 34: 666–71.
- Zou K, Ding G, Huang H. Advances in research into gamete and embryo-fetal origins of adult diseases. *Sci China Life Sci* 2019; 62: 360–8.
- Hann MC, Lau PE, Tempest HG. Meiotic recombination and male infertility: from basic science to clinical reality? *Asian J Androl* 2011; 13: 212–8.
- Enguita-Marruedo A, Sleddens-Linkels E, Ooms M, de Geus V, Wilke M, *et al*. Meiotic arrest occurs most frequently at metaphase and is often incomplete in azoospermic men. *Fertil Steril* 2019; 112: 1059–70.e3.
- Kubota H, Brinster RL. Spermatogonial stem cells. *Biol Reprod* 2018; 99: 52–74.
- Mulder CL, Zheng Y, Jan SZ, Struijk RB, Repping S, *et al*. Spermatogonial stem cell autotransplantation and germline genomic editing: a future cure for spermatogenic failure and prevention of transmission of genomic diseases. *Hum Reprod Update* 2016; 22: 561–73.
- Wu Y, Liang D, Wang Y, Bai M, Tang W, *et al*. Correction of a genetic disease in mouse via use of CRISPR-Cas9. *Cell Stem Cell* 2013; 13: 659–62.
- Hsu PD, Lander ES, Zhang F. Development and applications of CRISPR-Cas9 for genome engineering. *Cell* 2014; 157: 1262–78.
- Doudna JA, Charpentier E. Genome editing. The new frontier of genome engineering with CRISPR-Cas9. *Science* 2014; 346: 1258096.
- Wu Y, Zhou H, Fan X, Zhang Y, Zhang M, *et al*. Correction of a genetic disease by CRISPR-Cas9-mediated gene editing in mouse spermatogonial stem cells. *Cell Res* 2015; 25: 67–79.
- Sha Y, Zheng L, Ji Z, Mei L, Ding L, *et al*. A novel *TEX11* mutation induces azoospermia: a case report of infertile brothers and literature review. *BMC Med Genet* 2018; 19: 63.
- Adelman CA, Petrini JH. ZIP4H (*TEX11*) deficiency in the mouse impairs meiotic double strand break repair and the regulation of crossing over. *PLoS Genet* 2008; 4: e1000042.
- Yang F, Gell K, van der Heijden GW, Eckardt S, Leu NA, *et al*. Meiotic failure in male mice lacking an X-linked factor. *Genes Dev* 2008; 22: 682–91.
- Costoya JA, Hobbs RM, Barna M, Cattoretti G, Manova K, *et al*. Essential role of Plzf in maintenance of spermatogonial stem cells. *Nat Genet* 2004; 36: 653–9.
- Kanatsu-Shinohara M, Morimoto H, Shinohara T. Enrichment of mouse spermatogonial stem cells by melanoma cell adhesion molecule expression. *Biol Reprod* 2012; 87: 139.
- Kanatsu-Shinohara M, Ogonuki N, Inoue K, Miki H, Ogura A, *et al*. Long-term proliferation in culture and germline transmission of mouse male germline stem cells. *Biol Reprod* 2003; 69: 612–6.
- Zhang M, Zhou H, Zheng C, Xiao J, Zuo E, *et al*. The roles of testicular c-kit positive cells in *de novo* morphogenesis of testis. *Sci Rep* 2014; 4: 5936.
- Wang Y, Ding Y, Li J. CRISPR-Cas9-Mediated gene editing in mouse spermatogonial stem cells. *Methods Mol Biol* 2017; 1622: 293–305.
- Lander ES, Baylis F, Zhang F, Charpentier E, Berg P, *et al*. Adopt a moratorium on heritable genome editing. *Nature* 2019; 567: 165–8.



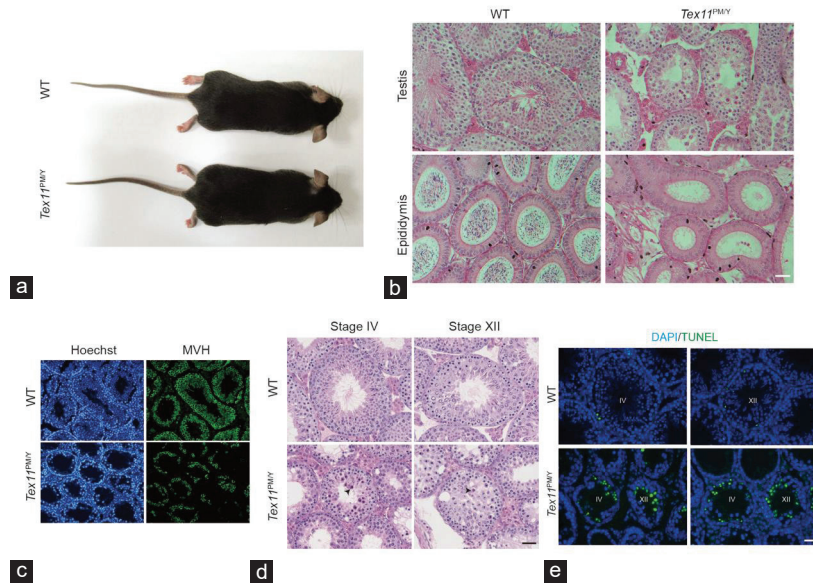
- 31 The Royal Society; National Academy of Sciences; National Academy of Medicine; International Commission on the Clinical Use of Human Germline Genome Editing. Heritable Human Genome Editing. Washington: National Academies Press (US); 2020.
- 32 Wen L, Liu Q, Xu J, Liu X, Shi C, *et al*. Recent advances in mammalian reproductive biology. *Sci China Life Sci* 2020; 63: 18–58.
- 33 Adashi EY, Cohen IG. Heritable Human Genome Editing: The International Commission Report. *JAMA* 2020; 324: 1941–2.
- 34 Yan M, Li J. Combined application of CRISPR-Cas and stem cells for clinical and basic research. *Cell Regen* 2020; 9: 19.
- 35 Bae S, Park J, Kim JS. Cas-OFFinder: a fast and versatile algorithm that searches for potential off-target sites of Cas9 RNA-guided endonucleases. *Bioinformatics* 2014; 30: 1473–5.
- 36 Lynch M. Evolution of the mutation rate. *Trends Genet* 2010; 26: 345–52.
- 37 Chabot B, Stephenson DA, Chapman VM, Besmer P, Bernstein A. The proto-oncogene c-kit encoding a transmembrane tyrosine kinase receptor maps to the mouse W locus. *Nature* 1988; 335: 88–9.
- 38 Muzumdar MD, Tasic B, Miyamichi K, Li L, Luo L. A global double-fluorescent Cre reporter mouse. *Genesis* 2007; 45: 593–605.
- 39 Brinster RL, Zimmermann JW. Spermatogenesis following male germ-cell transplantation. *Proc Natl Acad Sci U S A* 1994; 91: 11298–302.
- 40 Kanatsu-Shinohara M, Ogonuki N, Iwano T, Lee J, Kazuki Y, *et al*. Genetic and epigenetic properties of mouse male germline stem cells during long-term culture. *Development* 2005; 132: 4155–63.
- 41 Wu X, Goodyear SM, Abramowitz LK, Bartolomei MS, Tobias JW, *et al*. Fertile offspring derived from mouse spermatogonial stem cells cryopreserved for more than 14 years. *Hum Reprod* 2012; 27: 1249–59.
- 42 Valli H, Phillips BT, Shetty G, Byrne JA, Clark AT, *et al*. Germline stem cells: toward the regeneration of spermatogenesis. *Fertil Steril* 2014; 101: 3–13.

This is an open access journal, and articles are distributed under the terms of the Creative Commons Attribution-NonCommercial-ShareAlike 4.0 License, which allows others to remix, tweak, and build upon the work non-commercially, as long as appropriate credit is given and the new creations are licensed under the identical terms.

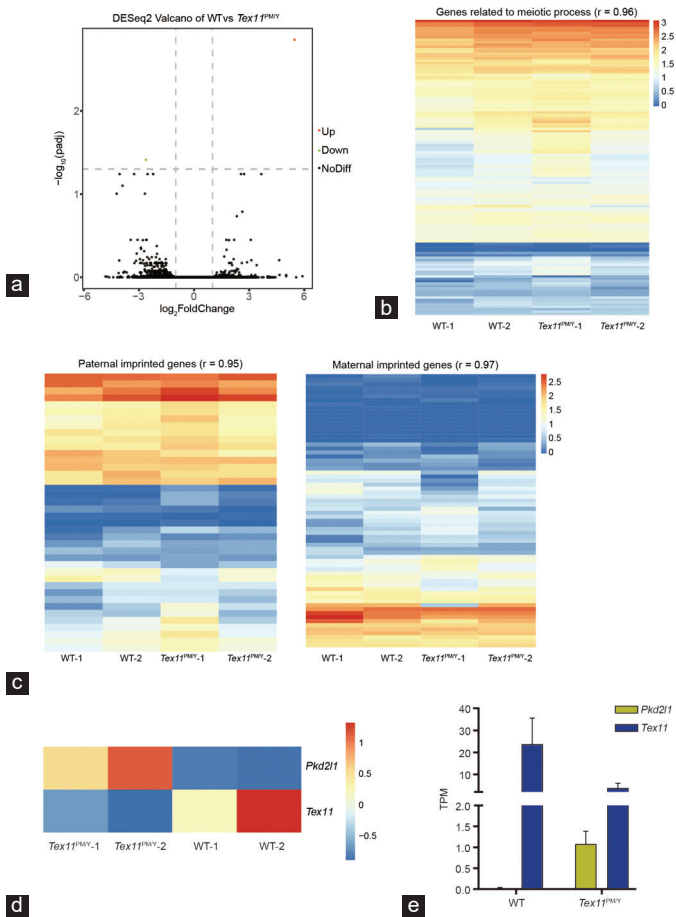
©The Author(s)(2021)



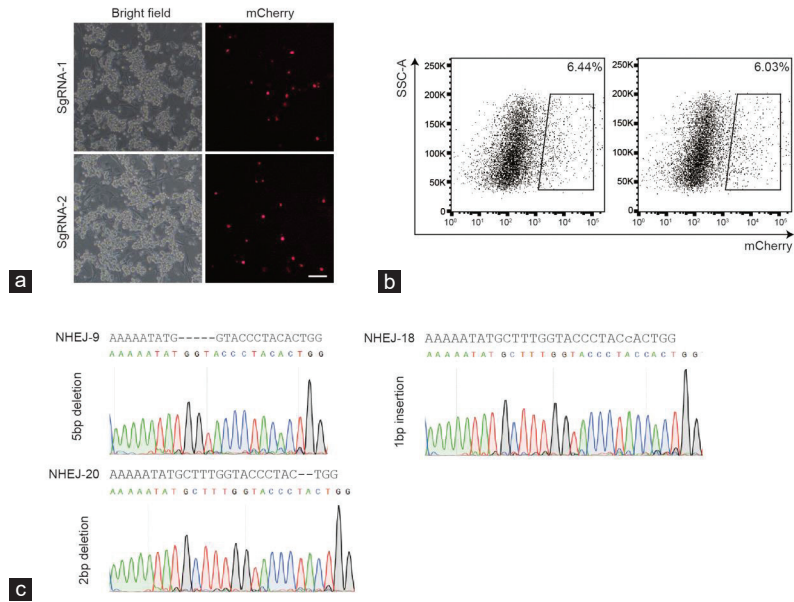
Supplementary Figure 1: Generation of mice carrying patient-derived *Tex11* mutation. (a) Alignment of TEX11 protein sequences. h., human; m. mouse. (b) Scheme for CRISPR-Cas9-mediated *Tex11* mutation in mice. SgRNAs were designed to target exon 16 of *Tex11*. The sgRNA-targeting sequence is shown in the upper line, and the PAM sequence is labeled in red. The sequence of donor oligo is shown under the gene, with 6 bp changes labeled in green. (c) Genotyping analysis of *Tex11*-mutant mice. (d) Morphology of WT and *Tex11*^{PM/+} female ovary, indicating normal growth and morphology. Scale bar = 25 mm. (e) Histological analysis of the ovary from WT and *Tex11*^{PM/+} mice, indicating normal oogenesis in *Tex11* heterozygous female. Scale bar = 100 μm. Two independent mutants were analyzed for each group. (f) Morphology of WT and *Tex11*^{PM/+} testis. Scale bar = 200 mm. (g) Histological analysis of the testis and epididymis from FO WT and *Tex11*^{PM/+} mice. Scale bar = 50 μm. WT: wild-type; *TEX11*: testis-expressed 11; CRISPR-Cas9: clustered regularly interspaced short palindromic repeats-CRISPR-associated endonuclease 9; sgRNA: single-guide RNA.



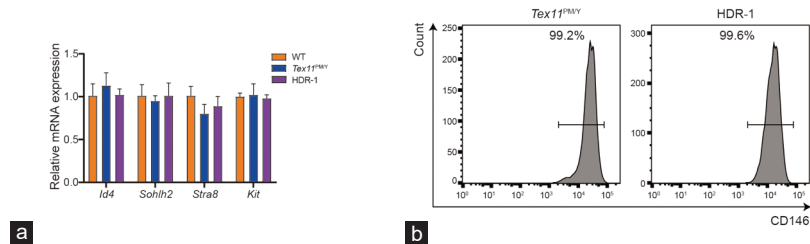
Supplementary Figure 2: Meiotic arrest in *Tex11*^{PMY} testis. (a) Image of 8-week-old WT and *Tex11*^{PMY} mice, indicating normal development of *Tex11*^{PMY} mice. (b) Histological analysis of the testis and epididymis of FO WT and *Tex11*^{PMY} mice. Scale bar = 50 μm. (c) Immunostaining of MVH in testicular sections from 8-week-old WT and *Tex11*^{PMY} mice with nuclei counterstained with Hoechst. Blue: Hoechst; Green: MVH. Scale bar = 50 μm. (d) Histological analysis shows apoptosis cells in stage IV and XII seminiferous tubules. Scale bar = 50 μm. (e) TUNEL staining shows apoptosis cells in stage IV and XII seminiferous tubules. Scale bar = 50 μm. WT: wild-type; TUNEL: terminal deoxynucleotidyl transferase biotin-dUTP nick end labeling.



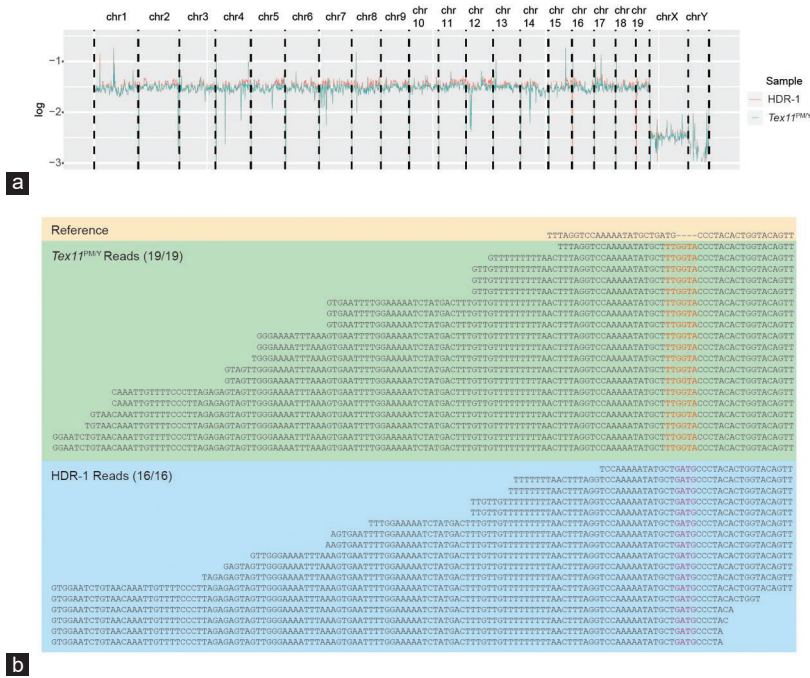
Supplementary Figure 3: *Tex11^{PMY}* SSCs display normal transcriptional profiles. (a) The volcano plot depicting the fold differences in gene expression levels between the WT and *Tex11^{PMY}* SSCs. Colored points refer to the differentially expressed transcripts according to fold change and P -value. (b) Heatmap correlation of \log_{10} genes related to meiotic process in WT and *Tex11^{PMY}* SSCs (r is the Pearson's correlation coefficient). (c) Heatmap correlation of \log_{10} imprinted genes in WT and *Tex11^{PMY}* SSCs. (left, paternal imprinted genes; right, maternal imprinted genes; r is the Pearson's correlation coefficient). (d) A heatmap of \log_{10} gene expression for the two differentially expressed genes. (e) Average gene expression level of the two differentially expressed genes. y axis, TPM from RNA-Seq data. WT: wild-type; SSCs: spermatogonial stem cells; RNA-Seq: RNA sequencing.



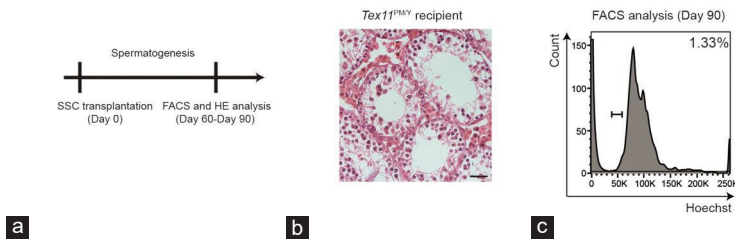
Supplementary Figure 4: Correction of *Tex11* mutation via CRISPR-Cas9-mediated gene editing in *Tex11^{PM/YY}* SSCs. (a) Lipofectamine-mediated CRISPR-Cas9 transfection in *Tex11^{PM/YY}* SSCs. Two sgRNAs were used for *Tex11* gene correction. mCherry indicating that SSCs successfully transfected with CRISPR-Cas9. Scale bar = 100 μ m. (b) SSCs with expressed Cas9 (co-expression of mCherry) were enriched through FACS, followed by single-cell expansion to obtain cell clones for *Tex11* gene analysis. (c) The sequences of *Tex11* gene in the SSCs lines carrying CRISPR-Cas9-induced NHEJ modifications. Small letters represent the inserted nucleotides. *TEX11*: testis-expressed 11; CRISPR-Cas9: clustered regularly interspaced short palindromic repeats-CRISPR-associated endonuclease 9; sgRNA: single-guide RNA; SSCs: spermatogonial stem cells.



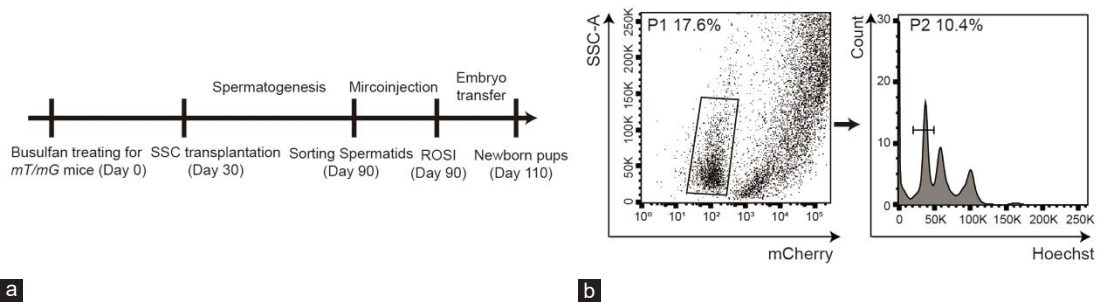
Supplementary Figure 5: Characterization of HDR-1 SSCs. (a) Expression of marker genes in *Tex11^{PM/YY}* and HDR-1 SSCs. The expression values were normalized to that of WT. The average values of three separate experiments are plotted. Significance was determined by two-tailed, unpaired Student's *t*-test. *Id4* and *Sohlh2* were used as undifferentiated marker genes, while *Kit* and *Stra8* were used as differentiated marker genes. (b) Flow cytometry analysis of CD146 in cultured *Tex11^{PM/YY}* and HDR-1 SSCs of passage 14, indicating that the majority of both *Tex11^{PM/YY}* and HDR-1 SSCs express CD146 during *in vitro* culture. WT: wild-type; HDR: homology-directed repair; SSCs: spermatogonial stem cells.



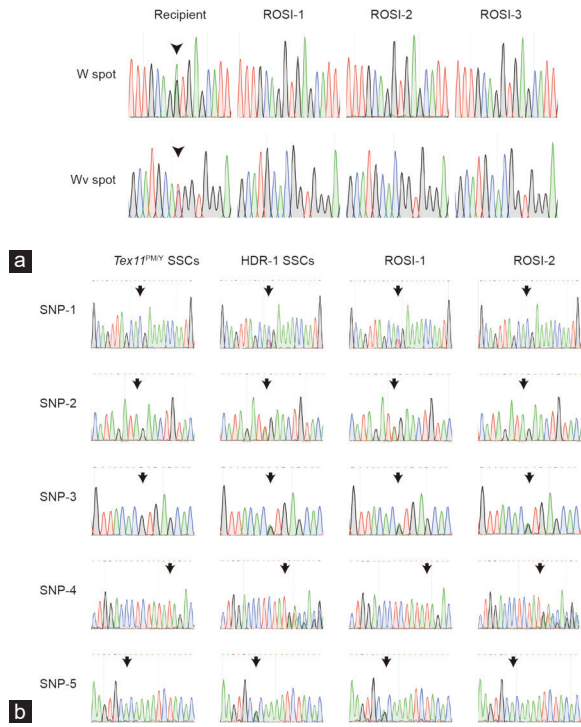
Supplementary Figure 6: WGS analysis of *Tex11^{PMY}* and HDR-1 SSCs. (a) Copy number of chromosomes in *Tex11^{PMY}* and HDR-1 SSCs, indicating normal karyotype of 40 chromosomes (38+X+Y) in both SSC lines. (b) Sequence analysis of *Tex11* in *Tex11^{PMY}* and HDR-1 SSCs. Each line represents a single read from WGS. *TEX11*: testis-expressed 11; SSCs: spermatogonial stem cells; HDR: homology-directed repair; WGS: whole-genome sequencing.



Supplementary Figure 7: Autotransplantation of HDR-1 SSCs into *Tex11^{PMY}* mice. (a) Diagram showing autotransplantation of HDR-1 SSCs into 3-week-old *Tex11^{PMY}* recipient mice ($n = 3$). Two months later, the testes were used for FACS and HE analysis. (b) Histological analyses of the *Tex11^{PMY}*-recipient testis, indicating no restoration of spermatogenesis. Scale bar = 40 μm . (c) FACS analysis of *Tex11^{PMY}*-recipient testis according to DNA content. SSCs: spermatogonial stem cells; HDR: homology-directed repair.



Supplementary Figure 8: Restoration of spermatogenesis following transplantation of HDR-1 SSC into busulfan-treated *mT/mG* recipients. (a) Diagram showing the repaired SSC lines derived from single SSCs without off-target mutations which are selected for transplantation into busulfan-treated *mT/mG* mice. Two months later, round spermatids were isolated from reconstituted testes and injected into mature oocytes to produce healthy mice carrying corrected *Tex11* gene. (b) Round spermatids are enriched from testicular cells of reconstituted testes. HDR-1 SSC-derived cells represented by RFP negative were enriched based on the expression of fluorescent protein and then subjected to DNA content analysis. SSCs: spermatogonial stem cells; HDR: homology-directed repair; *TEX11*: testis-expressed 11.



Supplementary Figure 9: Paternal origin of the ROSI-derived pups from *Kit^{fl}/Kit^{fl/y}* recipients. **(a)** Genotyping analysis of C-Kit in the newborn mice. Two peaks can be observed in the sequence of the control *Kit^{fl}/Kit^{fl/y}* mouse (indicated by arrowheads), while the HDR-1 SSC-derived mice have only one peak. **(b)** Genotyping analysis of selected SNPs 1–5 in the newborn pups. The SNP sites are indicated by arrowhead. SSCs: spermatogonial stem cells; HDR: homology-directed repair; ROSI: round spermatid injection; SNP: single-nucleotide polymorphism.

Supplementary Table 1: Primers used in this study

Primer name	Sequence (5'-3')	Application
GAPDH-QF	CACTCTCCACCTTCGATGC	Real-time PCR
GAPDH-QR	CTCTTGCTCAGTGCCTTGC	
<i>Tex11</i> -QF	TCCTACACATGTTTTCACTCGG	Genotyping of <i>Tex11</i> in mice and SSCs
<i>Tex11</i> -QR	CTGACCACCTGTAAAGCTCTG	
<i>Sohlh2</i> -QF	TCAAGGGGAGGAAGAGCGAT	Amplification of repair donor for SSCs transfection
<i>Sohlh2</i> -QR	TGTAACCTGGGCCATAATGG	
<i>Id4</i> -QF	GCCGTGAACAAGCAGGGTGA	Construction of sgRNA plasmid for SSCs transfection
<i>Id4</i> -QR	CTTGGAATGACAAGACGAGACG	
<i>Stra8</i> -QF	ACAACCTAAGGAAGGCAGTTTAC	Amplification of sgRNA transcription templates from PX330-mCherry
<i>Stra8</i> -QR	GACCTCCTCTAAGCTGTTGGG	
<i>Kit</i> -QF	CTAGCCAGAGACATCAGGA	Amplification of sgRNA transcription templates from PX330-mCherry
<i>Kit</i> -QR	CCATAGGACCAGACATCAC	
SgRNA-IVT-R	AAAAGCACCGACTCGGTGCCAC	Amplification of sgRNA transcription templates from PX330-mCherry
<i>Tex11</i> -IVT-F	TAATACGACTCACTATAGGGAATATGCTGATGCCCTACACGTTTTAGAGCTAGAAATAG	
<i>Tex11</i> -check F	ACTTAGGCTTCAAGTAAGTAGGCA	Genotyping of <i>Tex11</i> in mice and SSCs
<i>Tex11</i> -check R	TCACCTAAGTGCCACAGCAA	
<i>Tex11</i> -HDR-F	GACAGGAAGCCTCAACAGGG	Amplification of repair donor for SSCs transfection
<i>Tex11</i> -HDR-R	TGCTTCAGTGACAGGCCATT	
<i>Tex11</i> sgRNA-1F	CACC TTAGGTCCAAAAATATGCTT	Construction of sgRNA plasmid for SSCs transfection
<i>Tex11</i> sgRNA-1R	AAACAAGCATATTTTTGGACCTAA	
<i>Tex11</i> sgRNA-2F	CACC TATGCTTTGGTACCCTACAC	
<i>Tex11</i> sgRNA-2R	AAACGTGTAGGGTACCAAAGCATA	

SSCs: spermatogonial stem cells; HDR: homology-directed repair; GAPDH: glyceraldehyde-3-phosphate dehydrogenase; sgRNA: single-guide RNA; *Tex11*: testis-expressed 11.

Supplementary Table 2: Generation of mice carrying *Tex11* mutations via direct clustered regularly interspaced short palindromic repeat/associated endonuclease 9 cytoplasmic injection

Gene	Cas9/sgRNA (ng μ l ⁻¹)	Oligo Donor (ng μ l ⁻¹)	Number of injected zygotes	Number of 2-cell embryos	Number of newborn pups (dead)	Gender	Alive pups	Homo	Het
<i>Tex11</i>	100/50	100	150	131	33 (2)	Male	17	2	-
						Female	14	0	4

sgRNA: single-guide RNA; *Tex11*: testis-expressed 11

Supplementary Table 3: Summary of spermatogonial stem cell lines from single-cell expansion via clustered regularly interspaced short palindromic repeat-associated endonuclease 9-mediated gene correction of *Tex11*^{PMY} spermatogonial stem cells

SgRNA	Number of single cells used for expansion	Number of derived clones	Number of unedited clones (%)	Number of NHEJ clones (%)	Number of HDR clones (%)
SgRNA-1	580	17	4 (22.5)	10 (58.8)	3 (17.6)
SgRNA-2	580	16	11 (68.8)	5 (31.2)	0

HDR: homology-directed repair; SgRNA: single-guide RNA

Supplementary Table 4: The off-target analysis in repaired spermatogonial stem cell lines

Potential off-target site	Sequence	Mismatch bases	Mutant SSC lines (total)
chr1:66249826	TTAaGTaCAAAAATATGCaTTGG	3	0 (3)
chr1:102316146	TTAttTCaAAAAATATGCTTTGG	3	0 (3)
chr10:26854499	TaAaGTCCAAAAcATGCTTCGG	3	0 (3)
chr11:30465584	TcAGGTCCAAAcATtTGCTTAGG	3	0 (3)
chr12:42482925	TcAGGTCCAAAAATtGCcTAGG	3	0 (3)
chr12:79861136	caAGGTcCAAAAATATGCTTTGG	3	0 (3)
chr12:111449864	TcAGGTCCAAAAATAgGcTcTGG	3	0 (3)
chr14:114782600	TTAGtTtCcAAAATATGCTTTGG	3	0 (3)
chr2:73095017	TTAGtatCAAAAATATGCTTAGG	3	0 (3)
chr4:72841982	TTAGGTctAAAAAgATGtTTTGG	3	0 (3)
chr6:59018691	TTAGGaCCAAAAAgATcCTTAGG	3	0 (3)
chrY: 20249774	ccAGGTCCAAAAATtTGCTTAGG	3	0 (3)

The mismatch nucleotides were shown in lower cases. PAM is marked in red. No off-target nucleotides were detected in the potential off-target sites. SSC: spermatogonial stem cell

Supplementary Table 5: Summary of whole-genome sequencing analysis

	Raw reads	Clean reads	Clean bases	Rate (%)	Mapped reads	Properly paired	Properly paired reads	Base	Ratio (%)
<i>Tex11</i> ^{PMY}	763192270	747324824	109520937180	97.921	746464276	717938106	96.1	109393973559	99.884
HDR-1	836485138	824798254	121183737241	98.603	822262433	809857802	98.2	120809378500	99.691

HDR: homology-directed repair

Supplementary Table 6: Summary of genomic mutations in homology-directed repair-1

Region	SNV	Indels
Exon	0	0
Intron	15	3
Intergenic	21	3
Total	36	6

SNV: single-nucleotide variatio

Supplementary Table 7: Summary of single-nucleotide polymorphism sequence analysis of homology-directed repair-1 spermatogonial stem cell-derived pups

	<i>Chr</i>	<i>POS</i>	<i>REF</i>	<i>ALT</i>	<i>Mut (REF, ALT)</i>	<i>HDR-1 (REF, ALT)</i>	<i>C57</i>	<i>DBA</i>	<i>ROSI-1</i>	<i>ROSI-2</i>
SNP-1	chr6	132136304	G	A	14, 0	1, 17	G	G	G/A	G
SNP-2	chr5	5040740	A	T	35, 0	6, 17	A	A	A/T	A
SNP-3	chr15	31181191	C	T	24, 0	9, 22	C	C	C/T	C/T
SNP-4	chr17	21447226	TATA	T	31, 0	10, 23	TATA	TATA	TATA	T/TATA
SNP-5	chr12	89104845	T	C	36, 0	11, 26	T	T	C/T	T

As *Tex11^{PMY}* and HDR-1 SSCs were derived from C57 and DBA mixed background, unique HDR-1 SNP sites obtained during *in vitro* culture different from both *Tex11^{PMY}* SSCs and C57/DBA sequence were selected for analysis. For each SNP, genome of WT C57/DBA tails, *Tex11^{PMY}* and HDR-1 SSCs were subjected to PCR and sanger sequence. SNP-1/2/3/5 was detected in the HDR-1 SSC-derived pup ROSI-1, while SNP3/4 in the ROSI-2. SNP: single-nucleotide polymorphism; HDR: homology-directed repair; SSCs: spermatogonial stem cells; ROSI: round spermatid injection

Supplementary Table 8: Summary of offspring obtained from 4 male mice derived from homology-directed repair-1 spermatogonial stem cells

	<i>1st litter</i>	<i>2nd litter</i>	<i>3rd litter</i>
RO-M-1	3	5	9
RO-M-2	3	8	7
RO-M-3	6	7	-
RO-M-4	4	8	